TGGCAGCAACGGCTCCATGACTCCCAGCACAG (40-nucleotide oligomer, sense strand) for iNOS and TGAGACCTTCAACACCCCAGCCATGTACGTTG-CTATCCAG (40-nucleotide oligomer, sense strand) for β-actin. Filters were prehybridized and hybridized in Church and Gilbert hybridization solution [G. M. Church and W. Gilbert, *Proc. Natl. Acad. Sci. U.S.A.* **81**, 1991 (1984)]. Hybridization was performed at 60°C for 12 to 14 hours. The membranes were washed twice in 2× saline sodium citrate (SSC) and 0.1% SDS at room temperature for 10 min. This was followed by high-stringency washes in 0.2× SSC and 0.1% SDS at 60°C for 15 min. The filters were exposed to phosphor screens for 2 to 10 hours. The counts per band were measured by phosphorimaging (Molecular Dynamics) and used to determine the relative ratios of the intensity of the iNOS band to that of the β-actin band.

24. B. Wildemann, M. Sasaki, V. I. Christov, T. M. Dawson, V. L. Dawson, unpublished observations.
25. The iNOS PCR products obtained by several reactions were assessed by nucleotide sequence analysis. Sequencing was performed by the Genetics Resources CORE Facility of the Johns Hopkins University School of Medicine, with the use of the fluorescent dideoxy chain termination method using an automated DNA sequencer (model 373A, Applied Biosystems, Foster City, CA).
26. D. A. Geller *et al.*, *Proc. Natl. Acad. Sci. U.S.A.* **90**, 3491 (1993).
27. Immunoblot analysis of iNOS, p24, gp41, gp120, and β-tubulin was performed as described [A. H. Sharp *et al.*, *Neuron* **14**, 1065 (1995)]. Briefly, tissues were homogenized in ice-cold 50 mM Hepes (pH 7.4) with 1 mM β-mercaptoethanol, 1 mM phenylmethylsulfonyl fluoride, 1 mM benzamide, leupeptin (10 mg/ml), pepstatin A (10 mg/ml), aprotinin (1 mg/ml), and 1 mM EDTA, and centrifuged at 100,000*g* for 60 min. Polyacrylamide gel electrophoresis (PAGE) on a 5 to 16% gradient was used to separate proteins. After electrophoresis, proteins were electroblotted onto nitrocellulose and incubated with antibody to macNOS (1:500; Transduction Laboratories, Lexington, KY); antibody to p24 (HIV-1) (1:1000; Intracel, Cambridge, MA); antibody to gp41 (1:250; Intracel); antibody to gp120 (HIV-1), which recognizes recombinant gp120 and native gp120 from extracts of HIV-1–infected cells in protein immunoblots (1:250, Intracel); and antibody to β-tubulin (1:10000; Sigma), respectively. For gp41 protein analysis, equivalent amounts of protein lysate prepared from each of the pellet fractions after a 60-min 100,000*g* spin were resolved with PAGE on a 4 to 20% gradient. SDS (0.1%) was added to the tris-glycine buffer and Tween 20 (0.1%) was added to the phosphate-buffered saline for rinsing steps. Immunoblots were developed by enhanced chemoluminescence (Kirkegaard & Perry, Gaithersburg, MD). The specificity of the antibody to gp41 was demonstrated by immunoblots assessing the entire molecular weight range of 14 to 211 kD. gp41 revealed a single band at 41 kD only in HIV-1–infected tissue. Bands were scanned (Molecular Dynamics), and relative ratios of the intensity of the bands to that of the β-tubulin band were calculated.
28. S. M. Toggas *et al.*, *Nature* **367**, 188 (1994); J. M. Hill *et al.*, *Brain Res.* **603**, 222 (1993).
29. D. C. Adamson, J. D. Glass, J. C. McArthur, T. M. Dawson, V. L. Dawson, unpublished observations.
30. Recombinant $gp41_{IIIB}$ (amino acids 1 through 241, Intracel), recombinant p24 (amino acids 1 through 189; Intracel), recombinant $gp120_{IIIB}$ (amino acids 1 through 516; Intracel), and recombinant $gp46_{HTLV-1}$ (amino acids 26 through 215; Intracel) were used to investigate the potential induction of iNOS and neurotoxicity in primary mixed neuronal-glial cultures. Previous studies indicate that nonglycosylated recombinant gp41, as well as soluble peptides of gp41, are capable of inducing cytokines in both human and rodent cultures in a manner similar to that of glycosylated gp41 [P. Koka *et al.*, *J. Neuroimmunol.* 57, 179 (1995); P. Koka *et al.*, *J. Exp. Med.* **182**, 941 (1995)]. Primary cortical cell cultures were prepared from fetal rats at gestational day 16 in a procedure modified from that previously described [V. L. Dawson, H. P. Brahmbhatt, J. A. Mong, T. M. Dawson, *Neuropharmacology* **33**, 1425 (1994)]. Briefly, the cortex was dissected and the cells were dissociated by trituration in modified Eagle's medium (MEM), 20% horse serum, 25 mM glucose, and 2 mM L-glutamine after a 30-min digestion in 0.027% trypsin in saline solution. The cells were plated on 15-mm multiwell plates coated with polyornithine. Four days after plating, the culture medium was changed to MEM, 5% horse serum, 25 mM glucose, and 2 mM L-glutamine without phenol red. At this time, each protein was added in the presence or absence of L-NAME or L-Arg. The cultures were maintained in an 8% CO_2, humidified, 37°C incubator. The growth medium was supplemented with 10 μl of 2M glucose twice per week during the course of the experiment. Toxicity was assayed 7 days after initiation of exposure to the appropriate protein by trypan blue exclusion (0.4% trypan blue in CSS) as described (*12*). At least two separate experiments with four separate wells were performed, with a minimum of 4000 to 12,000 neurons counted per data point. The data were collected by an observer blinded to the treatment protocol. After 7 days, 400 μl of media was removed for colorimetric analysis of nitrite formation and added to 400 μl of Greiss reagent containing 4.25% phosphoric acid, 9.7 μM D-naphthyl ethylenediamine, and 0.14 mM sulfanilic acid. The samples were vortexed and after 5 to 10 min were read on a spectrophotometer at an absorbance of 563. The sample concentration was determined against a nitrite standard curve. For immunoblot analysis of iNOS, equivalent amounts of cell lysate prepared from the culture cells were loaded on a 5% SDS-PAGE gel (Bio-Rad, Hercules, CA) in tris-glycine buffer under reducing conditions and were further assessed as described for iNOS and β-tubulin assessment in cortical brain tissue.
31. D. C. Adamson, T. M. Dawson, V. L. Dawson, unpublished observations.
32. D. C. Adamson, C. M. Zink, J. E. Clements, T. M. Dawson, V. L. Dawson, unpublished observations; T. E. Lane, M. J. Buchmeier, B. B. Watry, H. S. Fox, *Mol. Med.* **2**, 27 (1996).
33. L. Bo *et al.*, *Ann. Neurol.* **36**, 778 (1994); M.-L. Wong *et al.*, *Nature Med.* **2**, 581 (1996).
34. C. Powers *et al.*, *J. Virol.* **68**, 4643 (1994). Demented and nondemented patients with AIDS differ in brain-derived HIV-1 envelope sequences.
35. The authors thank S. H. Snyder and R. T. Johnson for insightful critiques and discussion, A. Schmidt for secretarial assistance, and T. Billiar for the human iNOS cDNA. Supported in part by the following grants from the USPHS: NS07392 (D.C.A.), NS22643 (J.D.G., J.C.M., V.L.D., and T.M.D.), AI35042 (J.C.M.), RR007222 (J.C.M.), and Clinical Investigator Development Awards NS01577 (J.D.G.) and NS01578 (T.M.D.). V.L.D. is also supported by the American Foundation for AIDS Research; J.C.M. by the Charles A. Dana Foundation; and T.M.D. by the American Health Assistance Foundation, International Life Sciences Institute, and a Paul Beeson Physicians Scholars in Aging Research Award.

3 September 1996; accepted 4 October 1996

Reduction of Voltage-Dependent Mg^{2+} Blockade of NMDA Current in Mechanically Injured Neurons

Lei Zhang,* Beverly A. Rzigalinski, Earl F. Ellis, Leslie S. Satin†

Activation of the *N*-methyl-D-aspartate (NMDA) subtype of glutamate receptors is implicated in the pathophysiology of traumatic brain injury. Here, the effects of mechanical injury on the voltage-dependent magnesium (Mg^{2+}) block of NMDA currents in cultured rat cortical neurons were examined. Stretch-induced injury was found to reduce the Mg^{2+} blockade, resulting in significantly larger ionic currents and increases in intracellular free calcium (Ca^{2+}) concentration after NMDA stimulation of injured neurons. The Mg^{2+} blockade was partially restored by increased extracellular Mg^{2+} concentration or by pretreatment with the protein kinase C inhibitor calphostin C. These findings could account for the secondary pathological changes associated with traumatic brain injury.

Evidence from animals and humans has shown that the extracellular level of the excitatory neurotransmitter glutamate is elevated after traumatic brain injury (*1*, *2*). Elevated glutamate contributes to delayed tissue damage, presumably through activation of Ca^{2+}-permeable NMDA receptor channels. Treatment with NMDA receptor-channel antagonists has been reported to limit neurological dysfunction and partially preserve the bioenergetic state of posttraumatic brain tissue (*1*, *3*). In vitro, delayed neurodegeneration produced by using a plastic stylet to mechanically injure neocortical neurons in culture is attenuated by the NMDA antagonists dextrorphan or D-2-amino-5-phosphonovalerate (*4*). Despite the suggested involvement of NMDA receptors in these secondary pathological changes, it is not known whether mechanical injury directly affects NMDA channel properties in neurons of the central nervous system. Furthermore, because Mg^{2+} deficiency exacerbates, and increased extracellular Mg^{2+} attenuates, the pathological outcome of posttraumatic brain tissue (*5*), we hypothesized that voltage-dependent Mg^{2+} block of NMDA receptor channels (*6*) might be altered in injured neurons.

To examine the effects of mechanical stretch injury on NMDA currents, we used the whole-cell patch clamp technique (*7*)

Department of Pharmacology and Toxicology, Medical College of Virginia, Virginia Commonwealth University, Post Office Box 980524, Richmond, VA 23298–0524, USA.

*Present address: University of Pennsylvania Medical Center, Philadelphia, PA 19104, USA.
†To whom correspondence should be addressed. E-mail: lsatin@gems.vcu.edu

to record agonist-activated current in cultured neonatal cortical neurons (8). A cell injury model was used to simulate the in vivo brain tissue deformation associated with mild to moderate traumatic brain injury (8). This in vitro model produces strain comparable to that produced by in vivo brain injury (8), but reduces the confounding variables such as ischemia, hypoxia, hyperkalemia, and widespread membrane depolarization encountered in animal-model studies of head injury (*1*, *3*, *5*).

NMDA (200 μM)-activated currents recorded from uninjured control neurons under voltage clamp in the presence of 2 mM extracellular Mg^{2+} showed a typical "J"-shape when plotted against membrane command potentials (Fig. 1A). The negative conductance observed below −40 mV is known to be due to Mg^{2+} block of NMDA receptors (6). In contrast, the current-voltage (I-V) relationship of stretched neurons was more linear, indicating reduced Mg^{2+} block of NMDA channels (Fig. 1A). The amplitude of NMDA current in stretched neurons increased by a factor of 1.7 ± 0.1 at −60 mV (n = 18) and a factor of 3.1 ± 0.3 at −80 mV (n = 22) compared with control cells (Fig. 1B). No significant difference was found in the I-V relation at membrane potentials more positive than −40 mV. The more linear I-V relationship seen in stretched neurons occurred as early as 15 min after stretching and lasted at least 6 hours.

Stretch-injured and control neurons did not differ in their median effective dosage (ED_{50}) for NMDA to activate inward currents at −40 mV or −80 mV. The ED_{50} for control cells was 58 ± 4 μM (n = 8), whereas for injured neurons, the ED_{50} was 55 ± 3 μM [n = 7; not significantly different (NS)]. Moreover, NMDA-activated currents were similar in amplitude between −40 mV and +40 mV in the two groups of neurons (n = 34). The input resistances measured at −40 mV before NMDA stimulation were 340 ± 56 megohms for control neurons (n = 15) and 358 ± 36 megohms for stretched neurons (n = 18; NS), suggesting cell membrane integrity was intact in stretched neurons. In support of this, 5.7-mm mechanical deformation has little or no effect on cell uptake of the vital dye propidium iodide or on the resting membrane potential under the present experimental conditions (8, 9). Furthermore, we observed no shift in the reversal potential of NMDA currents in the stretched neurons, suggesting that mechanical perturbation did not markedly alter the ionic selectivity of NMDA channels (n = 22).

To further quantify the sensitivity of NMDA currents to Mg^{2+} block, we obtained Mg^{2+} concentration-response relations for control and stretched neurons. The apparent median inhibitory constants (IC_{50}'s) for Mg^{2+} block at −80 mV were 78 μM for control neurons (n = 8) and 1575 μM for stretched cells (n = 7; $P < 0.05$) (*10*). With 50 mM extracellular Mg^{2+}, the maximum inhibition of NMDA currents in stretched cells was 56% of that in control cells (Fig. 1C). Thus, control and stretched neurons had different sensitivities to Mg^{2+} blockade, with the sensitivity of NMDA currents to Mg^{2+} significantly reduced in injured neurons.

Reduction of the voltage-dependent Mg^{2+} block of NMDA channels in stretched neurons suggested that activated NMDA channels might induce larger ionic fluxes, especially Ca^{2+} flux, than that of control cells at voltages close to their resting membrane potentials (~−62 mV) (9). To test this hypothesis, we measured the change in intracellular free calcium ($[Ca^{2+}]_i$) in control and stretched neurons after NMDA application, using the fluorescent Ca^{2+} indicator FURA-2 (Fig. 2) (*11*). In physiological solution containing 2 mM Mg^{2+} and 3 mM Ca^{2+}, the basal $[Ca^{2+}]_i$ was 88 ± 7 nM in control neurons (n = 14) and 84 ± 7 nM in neurons stretched 15 min prior to the basal reading (n = 15; NS), further suggesting that mechanical stretch of this magnitude did not disrupt membrane integrity. Application of 200 μM NMDA increased $[Ca^{2+}]_i$ to 104 ± 12 nM (n = 9) in control neurons, a 17% increase over the basal level. However, in stretched neurons, 200 μM NMDA increased $[Ca^{2+}]_i$ to 226 ± 23 nM, a 170% increase over basal levels (n = 15). The enhanced $[Ca^{2+}]_i$ increase observed in stretched neurons could be mimicked by applying 200 μM NMDA to control cells bathed in nominally Mg^{2+}-free solution (a 183% increase over a basal level of 81 ± 5 nM; n = 8). Pretreating stretched or control neurons with the noncompetitive NMDA antagonist MK 801 (1 μM) (*12*) for 3 to 5 minutes completely blocked the responses to NMDA. The changes in $[Ca^{2+}]_i$ observed after NMDA application did not depend on the activity of voltage-dependent Ca^{2+} channels, because inclusion of the Ca^{2+} channel blocker Cd^{2+} (0.1 mM) yielded similar results in both control (n = 3) and stretched neurons (n = 3). In addition, it is unlikely that $[Ca^{2+}]_i$ increased in the injured neurons because of impaired $[Ca^{2+}]_i$ buffering, as application of the Ca^{2+} ionophore ionomycin elevated $[Ca^{2+}]_i$ to equal amounts in both stretched and control neurons (*13*). Thus, the enhanced increase in $[Ca^{2+}]_i$ observed in stretched neurons was caused primarily by reduced Mg^{2+} blockade of NMDA channels.

A number of mechanisms could underlie the reduced voltage-dependent Mg^{2+} blockade of NMDA channels observed after mechanical stretch. Activation of protein kinase C (PKC) has been shown to potentiate

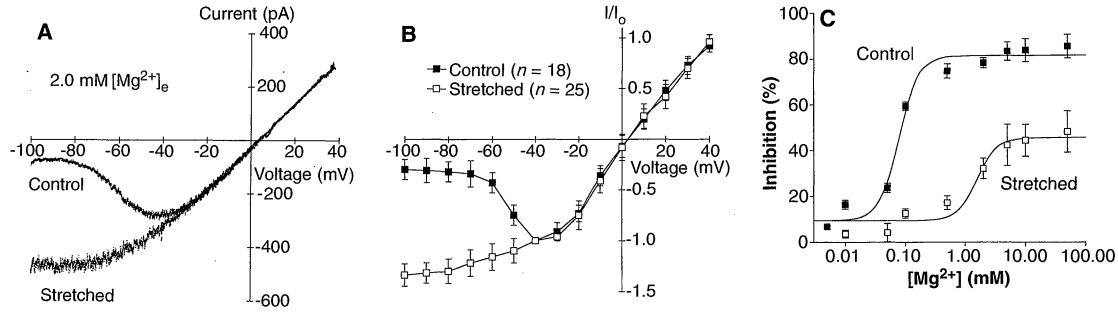

Fig. 1. Stretch-induced injury reduces voltage-dependent Mg^{2+} blockade of NMDA currents. (**A**) Whole-cell (*12*) NMDA currents recorded from representative control and stretched neurons plotted against linear voltage ramps from −100 mV to +40 mV of 6 s in duration in the presence of 2 mM extracellular Mg^{2+} ($[Mg^{2+}]_e$). Currents recorded in the presence and absence of NMDA (200 μM) were subtracted to generate NMDA currents. (**B**) Averaged current-voltage relationship of normalized NMDA currents from 18 control and 25 stretched neurons (mean ± SEM). For each neuron, current amplitudes at each command potential tested were normalized with respect to currents measured at −40 mV (I/I_o). The recording solution contained 2 mM Mg^{2+}. (**C**) The NMDA currents of control and stretched neurons differed in their sensitivity to extracellular $[Mg^{2+}]$. Means ± SEM of current inhibition by Mg^{2+} were plotted as a function of extracellular $[Mg^{2+}]$. Zero inhibition was defined as current amplitude at −80 mV recorded in nominally Mg^{2+}-free solution. All data points represent relative current amplitudes at −80 mV, and were fitted using AllFit, which simultaneously determined an optimal set of sigmoidal curves that best fit the experimental data (*10*). Maximal inhibition was 0.81 for control neurons and 0.45 for stretched neurons, whereas IC_{50} values for Mg^{2+} block were 78 μM for control cells (n = 7) and 1575 μM for stretched cells (n = 8).

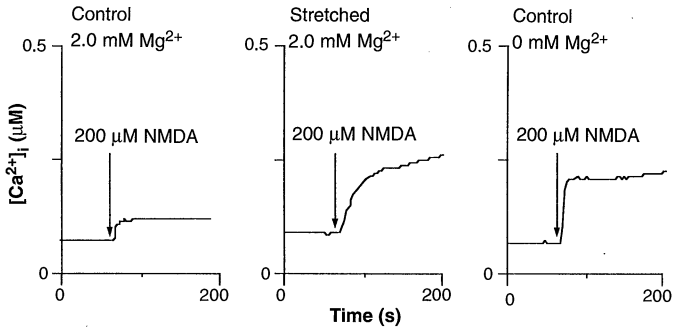

Fig. 2. Changes in $[Ca^{2+}]_i$ in control and stretched neurons after NMDA application. Traces are representative of the average response in 9 control cells and 15 stretched cells.

Mg^{2+} block of the channels in trigeminal neurons, and PKC inhibitors prevented the reduced Mg^{2+} block (*14*). In bladder smooth muscle, mechanical stretch activates several PKC isoforms (*15*). Thus, we tested whether the PKC inhibitor calphostin C could restore the Mg^{2+} block of NMDA channels in stretched neurons. Neurons were pretreated with calphostin C (100 nM) for 15 to 30 min before stretching. Treatment of control neurons with calphostin C shifted peak NMDA currents from -43.6 ± 1.3 mV ($n = 18$) to -38.4 ± 1.7 mV ($n = 5$), suggesting that NMDA receptor channels might be modulated by endogenous PKC activity under control conditions. There was no significant change in the reversal potential or the amplitude of the currents. Stretched neurons treated with calphostin C exhibited a 26.5% restoration of the voltage-dependent Mg^{2+} block at -80 mV and a 5.4% restoration at -60 mV ($n = 7$, Fig. 3). Thus, activation of PKC may contribute to the reduction of Mg^{2+} block of the NMDA current in stretched neurons.

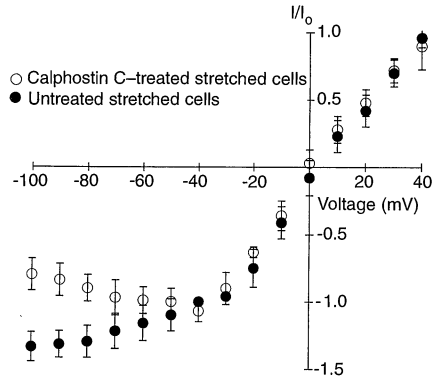

Fig. 3. Partial restoration of voltage-dependent Mg^{2+} block in stretched neurons pretreated with the PKC inhibitor calphostin C. After a 15- to 30-min incubation with 100 nM calphostin C, cells were stretched and then washed three times with recording solution. Treated noninjured neurons (not shown) were used to normalize the effects of calphostin C on treated injured cells. Injured untreated cells were used as controls. All data points represent mean ± SEM of relative current amplitude to current measurement at -40 mV (I/I_o).

In animal models of traumatic brain injury, infusion of $MgCl_2$ partially protects against neurological deficits (*5*). Our data suggest that one of the protective effects of increased extracellular Mg^{2+} may be through the partial restoration of Mg^{2+} blockade of NMDA receptor channels. In addition, increases in extracellular $[Mg^{2+}]$ may decrease glutamate release from central nerve terminals by blockade of voltage-gated Ca^{2+} channels. Conversely, decreased extracellular $[Mg^{2+}]$ in posttraumatic tissue exacerbates neurological dysfunction and increases mortality after brain injury (*5*). This may be attributed to enhanced Ca^{2+} influx through NMDA receptor channels due to their reduced Mg^{2+} blockade. Thus, there is a marked reduction of voltage-dependent Mg^{2+} block of NMDA currents after mechanical injury in central nervous system neurons, which in turn enhances NMDA-dependent Ca^{2+} influx and could explain the delayed neuronal excitotoxicity and pathological changes observed in traumatic brain injury.

REFERENCES AND NOTES

1. A. I. Faden, P. Demediuk, S. S. Panter, R. Vink, *Science* **244**, 798 (1989); Y. Katayama, D. P. Becker, T. Tamura, D. A. Hovda, *J. Neurosurg.* **73**, 889 (1990); P. Nilsson, L. Hillered, U. Ponten, U. Ungerstedt, *J. Cereb. Blood Flow Metab.* **10**, 631 (1990).
2. A. M. Palmer, D. W. Marion, M. L. Botscheller, D. M. Bowen, S. T. DeKosky, *Neuroreport* **6**, 153 (1994); R. Bullock *et al.*, in *Proceedings of the Ninth International Symposium on ICP and Brain Damage*, Nagoya, Japan, 16 to 19 May 1994, H. Nagai, K. Kamiya, S. Ishii, Eds. (Springer-Verlag, Tokyo, 1994), pp. 264–267.
3. R. L. Hayes *et al.*, *J. Neurotrauma* **5**, 287 (1988); T. K. McIntosh, R. Vink, H. Soares, R. L. Hayes, R. Simon, *J. Neurochem.* **55**, 1170 (1990); R. Bullock and H. Fujisawa, *J. Neurotrauma* **9**, S443 (1992); S. S. Panter and A. I. Faden, *Neurosci. Lett.* **136**, 165 (1992).
4. E. S. Tecoma, H. Monyer, M. P. Goldberg, D. W. Choi, *Neuron* **2**, 1541 (1989).
5. T. K. McIntosh, A. I. Faden, I. Yamakami, R. Vink, *J. Neurotrauma* **5**, 17 (1988); T. K. McIntosh, R. Vink, I. Yamakami, A. I. Faden, *Brain Res.* **482**, 252 (1989).
6. L. Nowak, P. Bregestovski, P. Ascher, A. Herbet, A. Prochiantz, *Nature* **307**, 462 (1984); M. L. Mayer and G. L. Westbrook, *J. Physiol. (London)* **361**, 65 (1985).
7. O. P. Hamill, A. Marty, E. Neher, B. Sakmann, F. J. Sigworth, *Pfluegers Arch.* **391**, 85 (1981).
8. Neuronal plus glial cell cultures were prepared from 1- to 2-day-old rats and plated in Flex Plates, which have a 2-mm thick silastic membrane bottom, as described [J. S. McKinney, K. A. Willoughby, S. Liang, E. Ellis, *Stroke* **27**, 934 (1996)]. After cells were cultured for 10 to 15 days, the silastic membrane was subjected to a rapid, reversible, 5.7-mm membrane deformation induced by a 50-ms pulse of air, as described [E. F. Ellis, J. S. McKinney, K. A. Willoughby, S. Liang, J. T. Povlishock, *J. Neurotrauma* **12**, 325 (1995)]. This degree of deformation produces 31% stretch, which is relevant to in vivo traumatic injury [D. Schreiber, T. A. Gennarelli, D. F. Meaney, in *Proceedings of the 1995 International Research Conference on Biomechanics of Impact*, Brunnen, Switzerland, 13 to 15 September 1995, A. Charpenne, Ed. (International Research Council on the Biokinetics of Impact, Lyon, France, 1995), pp. 233–244]. The electrophysiologic recording medium had a pH of 7.3 and an osmolarity of 285 mosM, and contained 130 mM NaCl, 4 mM KCl, 3 mM $CaCl_2$, 10 mM Hepes, 11 mM glucose, 0.01 mM glycine, and variable amounts of $MgCl_2$, added isoosmotically to the medium. The pipette solution contained 135 mM Cs-aspartate, 5 mM KCl, 2 mM NaCl, 0.2 mM $CaCl_2$, 10 mM EGTA, 10 mM Hepes, 2 mM Mg-ATP, and 0.6 mM guanosine triphosphate (pH 7.2). Spontaneous activity and synaptic transmission were reduced by 0.5 μM tetrodotoxin, 10 μM bicuculline, and 10 μM nimodipine. Data were acquired on a Macintosh Quadra 800 computer with an Instrutech ITC-16 computer interface and Pulse Control, version 4.3 J. Herrington and R. J. Bookman, *Pulse Control v 4.3: Igor XOPS for Patch Clamp Data Acquisition* (Univ. of Miami Press, Miami, 1994)] and Igor Pro, version 3 (Wavemetrics, Lake Oswego, OR) software. Currents were filtered at 1 kHz and digitized at 2 kHz.
9. S. J. Tavalin, E. F. Ellis, L. S. Satin, *J. Neurophysiol.* **74**, 2767 (1995).
10. A. DeLean, P. Munson, D. Rodbard, *Am. J. Physiol.* **235**, E97 (1977).
11. In order to measure $[Ca^{2+}]_i$, we loaded cultured neurons with 5 μM FURA-2 AM (in culture medium) for 1 hour at 37°C. After injury, cells were washed three times with external recording solution to remove unincorporated FURA-2. We measured $[Ca^{2+}]_i$, using a Ratiomaster System (Photon Technology International, South Brunswick, NJ) with a scanning monochrometer set to alternating excitation wavelengths of 350 and 380 nm. Emission was measured at 510 nm. Spectrophotometric measurements were recorded in situ in the Flex Plates by use of a Zeiss Achroplan 20× water immersion lens. Field size was adjusted to isolate one to three individual neurons. After recording a 2- to 3-min basal calcium level, neurons were stimulated with 200 μM NMDA as indicated. The $[Ca^{2+}]_i$ was calculated as described [G. Grynkiewicz, M. Poenie, R. Y. Tsein, *J. Biol. Chem.* **260**, 3440 (1985)]. FURA-2 is highly selective for Ca^{2+} over Mg^{2+}, with a Ca/Mg selectivity of >40,000. Thus, it is unlikely that the greater $[Ca^{2+}]_i$ responses to NMDA in injured cells reflect injury-induced alterations in neuronal $[Mg^{2+}]_i$.
12. C. J. McBain and M. L. Mayer, *Physiol. Rev.* **74**, 723 (1994); J. E. Huettner and B. P. Bean, *Proc. Natl. Acad. Sci. U.S.A.* **85**, 1307 (1988).
13. Application of 0.01, 0.1, or 1 μM ionomycin increased control cell ($n = 3$–4) $[Ca^{2+}]_i$ from a basal concentration of 82 ± 4 nM to 113 ±7 nM, 205 ± 13 nM, and 858 ± 50 nM (mean ± SEM), and stretched cell ($n = 3$–4) $[Ca^{2+}]_i$ from a basal concentration of 88 ± 4 nM to 126 ± 12 nM, 236 ± 21 nM, and 789 ± 52 nM, respectively (NS).
14. L. Chen and L. M. Huang, *Nature* **356**, 521 (1992).
15. K. Persson, J. J. Sando, J. B. Tuttle, W. D. Steers, *Am. J. Physiol.* **269**, C1018 (1995).

16. We thank S. Tavalin, J. Woodward, and T. Mirshahi for helpful discussions. We also thank J. McKinney, K. Willoughby, and S. Moore for the cell cultures; D. Compton for help with curve fitting; J. Povlishock and B. Lyeth for comments on the manuscript; and S. Holt for assistance with manuscript preparation. Supported by NIH Training Grant HL07537-14 (L.Z.) and Jacob Javits Neuroscience Investigator Award NS 27214 (E.F.E.). This work was supported in part by a Center of Excellence Grant-in-Aid from the Commonwealth of Virginia to J. Povlishock.

5 June 1996; accepted 8 October 1996